약학석사학위논문

The role of Transmembrane 4 L6 family member 5 in the development of zebrafish

Zebrafish 의 발달과정에서 TM4SF5 의 기능 연구

2013 년 2 월

서울대학교 대학원

약학과 의약생명과학전공

최 윤 주

Abstract

The role of Transmembrane 4 L6 family member 5 (TM4SF5) in zebrafish development

Yoon-Ju Choi

College of pharmacy

The Graduate School

Seoul National University

Transmembrane 4 L6 family member 5 (TM4SF5), a member of tetraspanin L6 superfamily, is a glycoprotein which has four transmembrane domains. TM4SF5 has been reported to be closely involved in tumorigenesis, being a signaling regulator during communication between tumor cells and tumor microenvironment via interaction with various proteins such as growth factor receptors, integrin receptors. It has been shown that TM4SF5 regulates important cellular processes like epithelial-to-mesenchymal transition (EMT), which is importantly functional for development of live fibrosis, tumorigenesis, and cell migration/invasion. In zebrafish, somitogenesis and myotome formation are the processes that a wide

range of cellular processes including cell migration/adhesion, EMT and morphological changes occur simultaneously. However, the function of TM4SF5 during embryogenesis in which EMT and cell migration/adhesion are crucial remains unknown. Here we investigated the function of TM4SF5 in zebrafish embryogenesis.

Expression of *tm4sf5* mRNA was elevated during somitogenesis, and deteced in porsterior somites. After 1 dpf, *tm4sf5* transcripts were detected in whole myotome. Knock-down of *tm4sf5* using morpholino oligonuceotides resulted in an aberrant development of trunk and abnormal morphology of muscle fibers. The overall muscle mass was also reduced in *tm4sf5* morphants. In addition, the knock-down of tm4sf5 altered expression of integrin α5, which is known to be expressed in muscle pioneer and necessary for somite boundary maintenance. Because the somite boundaries mature into myotome boundaries and necessary for proper morphogenesis of muscle fibers, we could infer that tm4sf5-dependentt integrin α5 expression or function is important for normal myotome formation. Taken together, these observations suggest that TM4SF5 plays a regulatory role in zebrafish embryogenesis, especially in myogenic processes, presumably via collaborations with integrin α5.

Keyword : development, TM4SF5, zebrafish, myotome, muscle, integrin α5

Student number : 2011-21775

CONTENTS

LIST OF FIGURES

Introduction

Transmembrane 4 L6 family member 5 (TM4SF5) is a transmembrane protein, which has four transmembrane domains. It has a conserved tetraspanin L6 domain, characterized with two cysteine residues instead of four cysteine residues in classical tetraspanins. TM4SF5 is upregulated in multiple types of cancers, and closely related in tumorigenesis. It has been shown to act as a regulator in tumor microenvironment via crosstalk with integrins (1-3). TM4SF5 expression in hepatocytes induces cell surface retention of integrin α5, and activation of downstream molecules like focal adhesion kinase (FAK)/c-Src (2). It has also induces VEGF secretion, resulting in elevated angiogenic activity of neighboring endothelilal cells (2). TM4SF5 modulate actin organization and focal adhesion dynamics via interaction with integrin α2 (3). Cell migration/invasion is enhanced by TM4SF5-mediated FAK activation (4). Recent study shows that TM4SF5 directly bind FAK dependent on adhesion signals, indicating TM4SF5 as a regulator of cell migration (5). Importantly, TM4SF5 is able to induce epithelial-to-mesenchymal transition (EMT) in hepatocytes through regulation of cytosolic $p27^{kip1}$, inhibiting RhoA pathway (6). Cells overexpressing TM4SF5 present loss of cell-cell contact, downregulation of epithelial cell markers such as E-cadherin and ZO-1 (6). TM4SF5 expression caused by smad activation of TGF-β1 can also drive EMT in cells (7).

Epithelial-to-mesenchymal transition (EMT) is the process that epithelial cells lose its epithelial characters and gain mesenchymal traits, including increased cell motility and loss of cell-cell contact (8). It is the phenomenon including alteration

in cell morphology, cell migration and adhesion capacity (8). When EMT occurs, epithelial marker proteins like E-cadherin and ZO-1 are decreased, and mesenchymal marker proteins like N-cadherin, vimentin, and fibronectin are increased (9). The concept of EMT first emerged as an important process in embryogenesis, and now it is described in tissue fibrosis, metastatic tumor cells, and many other diseases (8). In previous studies, the evidences that TM4SF5 can induce EMT in hepatocytes leading to development of fibrotic phenotypes (10) and cellular elongation, contact inhibition loss, and enhanced migration/invasion were presented (6, 7). Thus, we infer that TM4SF5 is also able to function in EMT process during embryogenesis, regulating cell migratory mechanisms.

During embryonic morphogenesis, cells go through a series of complicated movements and cell-shape changes to form highly ordered structures in exact time and position. In these processes, a variety of intracellular signaling cascades are activated to regulate migration, adhesion, and morphological changes (11). In terms of developing animal, the study of molecular events involved in modulation of cell motility and cell-shape change is useful because these biological events occur simultaneously and closely interconnect (11). One of the well-studied examples is the formation of the vertebrate myotome including the segmentation of somites (12). In all vertebrates, somites are mesodermal derivatives generated as transient structures along the anterior-to-posterior body axis during segmentation period (12). The somitic cells undergo a wide range of migration and morphological changes and give rise to dermatome, sclerotome, and myotome (12). Unlike other vertebrates, in zebrafish, the majority of somitic cells differentiate into muscle, forming comparatively large myotome (13). Because of this feature, zebrafish is

used as an important animal model for the study of cellular mechanism in myotome formation. Here we used zebrafish as an animal system to pursue the study.

Zebrafish, *Danio rerio*, is widely used for scientific researches nowadays. It has many advantages over any other vertebrates. Zebrafish embryos have transparent body enabling various method of microscopic observation, go through rapid development, and can be raised with lower cost of maintenance (14). Also due to the high fecundity of female embryos, several hundreds of embryos can be obtained by a single fertilization (14). In addition to these features, genetic method such as gene-knockout or mutagenesis is easily applied to the embryos compared with mouse developmental genetics (14).

At the first day of zebrafish embryonic development, somitogenesis is nearly over and myotome begins to mature (15). Within the segmented part of somites, cells composing the posterior compartment begin to express myogenic transcription factors, such as *myoD* and *myf5* (16). These cells are adaxial cells located in mesoderm adjacent to the notochord, and shortly after somite formation, these adaxial muscle progenitor cells begin to differentiate into slow muscle fibers (15). Most of these cells migrate laterally across the myotome and elongate to form the superficial slow muscle fibers, with a few cells remaining medially referred as muscle pioneers (17). In the lateral part of adaxial cells, called as paraxial mesoderm, cells differentiate into fast muscle fibers (17). The elongation of slow muscle fibers is necessary for the elongation of fast muscle fibers (18). During these processes, the fibers elongate anchoring somite boundaries, composed of epithelial somitic border cells (19). The proper formation of somite boundaries is important for the normal elongation of muscle fibers (19). The somite boundaries

mature into myotome boundaries, growing V-shaped with accumulation of various extracellular matrix proteins (e.g. fibronectin) and focal adhesion components (e.g. FAK, integrin, and paxillin) (20, 21). Especially fibronectin matrix is assembled depending on integrins and it is crucial for boundary maintenance by acting on the epithelialization of somitic border cells (22). The accumulation of FAK, a downstream molecule of integrin signaling, is affected by integrin (20). In these molecular events related with myotome morphogenesis, the interaction of focal adhesion protein and membrane receptors is important but exact signaling mechanisms remain poorly understood.

Tetraspanins are known to interact with other tetraspanins, integrins, and other molecules to form large tetraspanin-enriched microdomains (TEMs) (23, 24). TEMs have been known to function as a signaling hub that mediates cell adhesion and migration (23, 24). Recently, tm4sf4, one of the other L6 family members, has been shown to affect cell migration in regulating pancreatic islet cell differentiation in the context of the development (25). However, it is unknown that how TM4SF5 functions in developmental process. As a member of tetraspanins and regulator of cell migration and EMT, we could hypothesize that TM4SF5 might get involved in the zebrafish morphogenesis via interaction with many other proteins.

As expected from the facts that the tetraspanin TM4SF5 is conserved in zebrafish and its binding domain for FAK is also conserved through data base screening, we found novel roles of *tm4sf5* in the development of zebrafish especially during myotome formation. The observations in the current study suggest that tm4sf5 might affect the normal expression of integrin α5 and function as a modulator in myogenic processes.

Material and method

1. Protein sequence analysis

TM4SF5 protein sequences for zebrafish (NP_001002372.1), mouse (NP_083636.2), and human (NP_003954.2) were obtained from the National Center for Biotechnology Information (NCBI). Multiple sequence alignment was performed using CLUSTAL Ω and the NCBI HomoloGene service.

2. Zebrafish strains and maintenance

Zebrafish (*Danio rerio*) were maintained at 28°C in an oxygenated fish tank on a 14/10 hr (light/dark) cycle as previously described (14) and used for the experiments in the study. Embryos were collected from natural mating and maintained in mineralized water. Ages are given in hours post fertilization (hpf) based on the standard developmental stage (15).

3. RNA isolation and cDNA synthesis from zebrafish embryos

Fifteen to thirty embryos matched with exact ages were collected in eppendorf tubes. With narrow-ended tip, the embryo solution was completely removed from the tubes. By adding 500 μl of Trizol reagent (Ambion) into the tubes and homogenizing with 1 ml syringe, Embryos were lysed completely. After 100 μl of chloroform was added and centrifuged at 4°C, 13,000 rpm for 15 min, supernatant was separated and moved into new tube. Then 250 μl of isopropanol was added

and centrifuged at 4°C, 13,000 rpm for 15 min. Pellet was collected and washed with DEPC-treated 75% ethanol. Finally total RNA pellet was eluted with 20 µl of DEPC-treated RNase free water 20 µl. All process was done at 4°C in RNase free environment.

From 1 µg total RNA, 20 µl of cDNA was synthesized. For 1 µg template RNA, 1 µl of oligo dT was added and incubated at 70°C for 5 min and then on ice for 5 min. After the reactant was mixed with 5X M-MLV reverse transcription buffer, 10 mM dNTP mixture (2.5 mM dUTP, dATP, dGTP, dCTP, dTTP at pH 7.0), Ribonuclease inhibitor, and M-MLV reverse transcriptase (Promega), total 20 µl of reaction mixture was incubated at 25°C, 5 min for annealing, at 42°C, 60 min for reverse transcription reaction, and at 70°C, 15 min for inactivation of the enzyme.

4. Polymerase chain reaction

From 1 µl aliquot of isolated cDNA, polymerase chain reaction was done according to the following process. PCR reaction was performed for 30 cycles on a multigene optimax thermal cycler. Reaction conditions include initial denaturation at 95°C for 5 min, cycling of 95°C for 50 sec, 55°C for 30 sec, 72°C for 50 sec, and then final extension at 72°C for 5 min.

The following primer pairs were used for RT-PCR analysis to confirm the effect of splice–blocking morpholino: F1 (5'-ATGTGTACCGGAAAGTGTGCT-3') was used for a forward primer. Reverse primers were followed; R1 (5'-TGTTGGATGTATCTAATCAGTTTTGT-3') giving a product of 363 bp, R2 (5'-CCTTTCCTGTCCTCAAATGGAT-3') giving a product of 398 bp, R3 (5'-GATTTTCTTTTCCGGCAGTCT-3') giving a product of 629 bp, and for control

experiment, β-actin forward (5'-GCAGAAGGAGATCACATCCC-3'), and β-actin reverse (5'-CATTGCCGTGCACCTTCACCG-3') giving a product of 323 bp were used. The primer pairs used for RT-PCR analysis of gene expression were followed. : *tm4sf5* forward (5'-GATAAGCTTATCATGTGTACCGGAAAGTG TGCT-3'), *tm4sf5* reverse (5'-GATTCTAGAATCCAGACCTCCTTCATCCGATT T-3'), *integrin α5* forward (5'-CCCAAGCTTTCGGCGTCTACAAGCTGCTCTC-3'), *integrin α5* reverse (5'-TGCTCTAGA AGGTCCTCCCAGCACCACCTT-3').

5. *In vitro* transcription of digoxygenin-UTP labeled anti-sense RNA probes

The following probes were used: *myod* (26), obtained from Kyungpook National University, T. Huh ph.D), *tm4sf5* (NM_001002372), *integrin α5* (NM_001004288). Each DNA was amplified to include restriction enzyme site by PCR reaction and eluted using PCR purification kit (GeneAll). The DNAs were then cloned into pGem-T vector (Promega). Sequences and directions of inserted DNAs were confirmed by direct sequencing and BLAST analysis provided by NCBI (National Center for Biotechnology Information). Probe vectors were linearlized by appropriate restriction enzyme at 5' or 3' end of each sequence. Completely restricted vectors were purified by Gel purification kit (GeneAll). *In vitro* transcription of digoxygenin-labeled RNA was carried out using Digoxygenin RNA labeling kit (Roche). Template DNA was removed by treating DNase I (Roche) at 37°C for 15 min. One μl of 0.5 M EDTA was added to finish the reaction. RNA was precipitated with 1 μl of 5 M ammonium acetate and

centrifuged with 35 µl of 100% ethanol at 4°C, 12,000 rpm. Supernatant was removed completely and pellet was centrifuged with 50 µl of 70% ethanol at 4°C, 12,000 rpm. After removal of the supernatant, pellet was eluted with 20 µl of formamide and stored in -20°C. The RNA probe was denatured at 80°C for 5 min before use.

6. Whole mount *in situ* hybridization

Whole mount *in situ* hybridization was carried out with digoxygenein-labeled antisense *in situ* probes as described previously (27).

6.1 Collection and fixation of the embryos

The day after mating the zebrafish embryos, the embryos matched with experimental ages were collected in eppendorf tubes. Then the embryos were fixed in 4% paraformaldehyde (Sigma) in PBS at 4°C overnight or 25°C for 4 hr. Embryos in the stages before 24 hpf were dechorinated before the fixation, and embryos after 24 hpf were fixed after dechorinated. The chorion was removed by using sharp forceps. Embryos to be used for *in situ* hybridization were grown in 0.003% (0.033 mg/ml in embryo medium) phenylthiourea to inhibit formation of pigmentation. Fixed embryos were washed with PBS-Tw (1X PBS, 0.1% Tween 20) twice and treated with 100% methanol at -20°C for at least 2 hr. In methanol, fixed embryos could be stored for several months. RNA grade solutions and apparatus were used.

6.2 Treatment of proteinase K and hybridization

Stored Embryos (twenty to fifty embryos/tube) in 100% methanol were rehydrated in 75%, 50%, 25% methanol in PBS-Tx buffer (1× PBS, 0.1% Triton X-100) serially. After three times of washing with PBS-Tx buffer, embryos were treated with 300 µl/tube of 10 µg/ml proteinase K (GenDEPOT) in PBS-Tx; 10 min for 24 hpf embryos, 15 min for 48 hpf embryos, 30 min for 96 hpf embryos. Then the embryos were fixed with 4% paraformaldehyde (Sigma) in PBS at room temperature for 20 min. After three times of washing with PBS-Tx buffer, embryos were pre-hybridized in HB4* buffer (50% formamide, 5X SSC and 0.1% Tween-20, at pH 7.0 with citric acid) for over 2 hr at 65°C. Afterwards the buffer was replaced by fresh HB4 buffer (HB4* with 5 mg/ml torula RNA, 50 µg/ml heparin) containing digoxygenin-labelled RNA probe at 50 ng final concentration and incubated overnight at 65°C with gentle shaking.

6.3 Anti-Digoxygenin antibody reaction and staining

After hybridization, the embryos were washed at 65°C by shaking for 10 min. Each washing was done as following with changes of wash buffers (75% HB4*, 25% 2XSSC; 50% HB4*,50% 2XSSC; 25% HB4*, 75% 2× SSC). Then washing was done twice for 30 min with 0.2× SSC. Followed by 10 min washes at room temperature with: 75% 0.2× SSC, 25% PBS-Tw (1× PBS, 0.1% Tween-20); 50% 0.2× SSC, 75% PBS-Tw, and finally 100% PBS-Tw. Throughout these series of washes, the residual RNA probe was removed. Before treatment of anti-digoxygenin-alkaline phosphatase Fab (Roche), embryos were incubated in glycine buffer (0.1 M glycine at pH 2.2, 0.1% Tween-20) to remove endogenous alkaline phosphatase. Blocking steps to prevent nonspecific binding were

performed in blocking buffer (5% sheep serum in PBS-Tw) at room temperature over 3 hr. Then the blocking solution was changed with anti-DIG-AP Fab solution (diluted 1:4000, with 5% sheep serum in PBS-Tw) and incubated at room temperature over 4 hr or at 4°C overnight. The embryos were washed in several changes of PBS-Tw during 5 hr followed by 3 washes 5 min, 10 min, 20 min each in staining solution (100 mM Tris-HCl at pH 9.5; 50 mM $MgCl_2$, 100 mM NaCl, 0.1% Tween-20) and stained by adding BCIP/NBT stock solution (Roche) at 18.6 µl/ml. The staining reaction was stopped by several changes of PBS-Tw. The embryos were stored at 4°C in 90% glycerol/PBS and photographed or sectioned.

7. Whole mount *in situ* immunostaining

One dpf zebrafish embryos were fixed in 4% paraformaldehyde in PBS at 4℃ overnight, rinsed over 2 hr with PBS-Tw, treated with collagenase (1 mg/ml) in PBT for 10 min, quickly washed with PBT twice, PBDTT (1× PBS, 0.1% Tween 20, 1% DMSO, 1% BSA, 0.5% Triton X-100) twice, and then blocked in PBDTT with 5% BSA, 10% sheep serum at room temperature for 3 hr. Primary antibody to F59 (anti-myosin heavy chain antibody to detect slow muscle cells) and F310 (anti-myosin light chain antibody that labels fast-twitch muscle myosin) was added at 1:10 dilution and incubated overnight at 4℃. Embryos were washed over 4 hr at room temperature in PBDTT, and blocked in PBDTT with 1% BSA 4 hr at room temperature. Biotin-labeled anti-mouse IgG (Vector laboratories) was added at 1:2000 dilution and incubated overnight at 4℃. After wash with PBDTT over 4 hr at room temperature, vectastain ABC reagent (Vector laboratories) was added to embryos and incubated according to manufacturer's instructions. After the second

washing with PBDTT over 2 hr, diaminobenzidine and H_2O_2 was added as manufacturer's instructions. After color detection was over, embryos were fixed with 4% paraformaldehyde in PBS for 20 min at room temperature. For microscopy and storage, embryos were washed with PBT, and stored in PBT with 90% glycerol. Images were collected on a microscope (BX51, Olympus).

8. Anti-sense morpholino oligonucleotides

Morpholino-modified oligonucleotides (MO) were purchased from Gene-tools (Philomath, OR). The sequences of the MO were targeted against the splice-donor site of exon 1 of *tm4sf5* (MO1-ACAGACTGGAAACTCACAAATAGTC) and translation initiation site of *tm4sf5* (MO2-TACACATGGCCTTTCACACGAGC CA). MOs were stored at concentration of 1 mMole stock at -80℃. Embryos were microinjected at the 1-4 cell stage with 2, 3, or 4 ng morpholino/embryo as described previously (28). Standard control morpholino was used at the respective concentration.

9. Cryosection

Embryos hybridized with *tm4sf5* RNA probe and stored at 4°C in 90% glycerol/PBS were used for cryosection. After removal of glycerol by several washes in TBS-Tw, 5-10 embryos were transferred to plastic mold filled with Frozen section media (FSC22 Clear, Leica) and oriented appropriately with forceps. Then the embryos were stored at -80°C overnight. Using Microm cryostat HM525 (Thermo scientific), serial sections (10 μm thick) were cut. Sectioned slices were

attached on microslides and visualized with a microscope (BX51, Olympus). A filter for DIC was used for imaging.

10. Microscopy

Morphology of embryos were viewed by using Zeiss Axiocam ICc1 microscope (Carl Zeiss) and processed with Axiovision software. Images after performing immunohistochemistry and section were obtained with BX51 microscope (Olympus).

Result

1. Comparison of TM4SF5 protein sequence homology from zebrafish and other vertebrates.

Zebrafish *tm4sf5* gene is located in chromosome 7. The full-length clone of zebrafish *tm4sf5* is 1,672 bp and consists of a reading frame encoding 201 amino acids. We first analyzed sequence homology of TM4SF5 protein among zebrafish and other vertebrates through data base screening. Approximately fifty-seven percent of amino acids in zebrafish TM4SF5 are identical with human and mouse TM4SF5 (Fig. 1A). Importantly, several regions are highly conserved, including the NH_2-terminal region (met-1 to cys-9; 8 of the 9 amino acids identical), and the intracellular loop domain (arg-67 to val-89; 22 of the 23 amino acids identical) (Fig. 1B). The intracellular loop domain (ICL) of TM4SF5 has been known to directly bind focal adhesion kinase (FAK) (5). The ICL of TM4SF5/FAK interaction is necessary for FAK activation and affects cell migration or adhesion.

During embryogenesis, cells undergo dynamic changes of migratory and adherent states. So these similarities in protein sequences indicate that zebrafish TM4SF5 might also have roles in developmental processes through molecular interactions or regulation of cell migration in a similar way to human.

A

	H.s_TM4SF5	M.m_TM4SF5	D.r_TM4SF5
H.s_TM4SF5	100%	82.7%	57.6%
M.m_TM4SF5		100%	56.5%
D.r_TM4SF5			100%

B

Figure 1. Comparison of TM4SF5 protein sequence homology between zebrafish and other vertebrates.

(A) Percentage identities among *H. sapiens, M. musculus, D. rerio*. *D. rerio* TM4SF5 has a 57.6% homology with *H. sapiens*. (B) CLUSTAL Ω species alignment between human, mouse, and zebrafish TM4SF5. Identical(*), highly conserved(:), and weakly conserved(.) Highly conserved regions are highlighted in sky blue color.

2. Expression of *tm4sf5* during zebrafish development

2.1 RT-PCR analysis of *tm4sf5*

Performing RT-PCR analysis, we revealed that *tm4sf5* mRNA level showed several peaks during zebrafish development. The expression level of *tm4sf5* showed a spike at 17-18 hpf, decreased until 2 dpf, and increased again at 3 or 4 dpf (Fig. 2A). Because the most parts of morphogenesis in zebrafish embryos are completed by 3 dpf, we investigated the first peak of *tm4sf5* expression more thoroughly. The first spike in expression (17-18 hpf) corresponds to a time period at which somites are formed and developed into the myotome (15). In the more detailed time-wise analysis, *tm4sf5* expression was initiated in gastrulation period (90% epiboly), increased at the beginning of somitogenesis, and maintained throughout the somitogenesis stage (Fig. 2B).

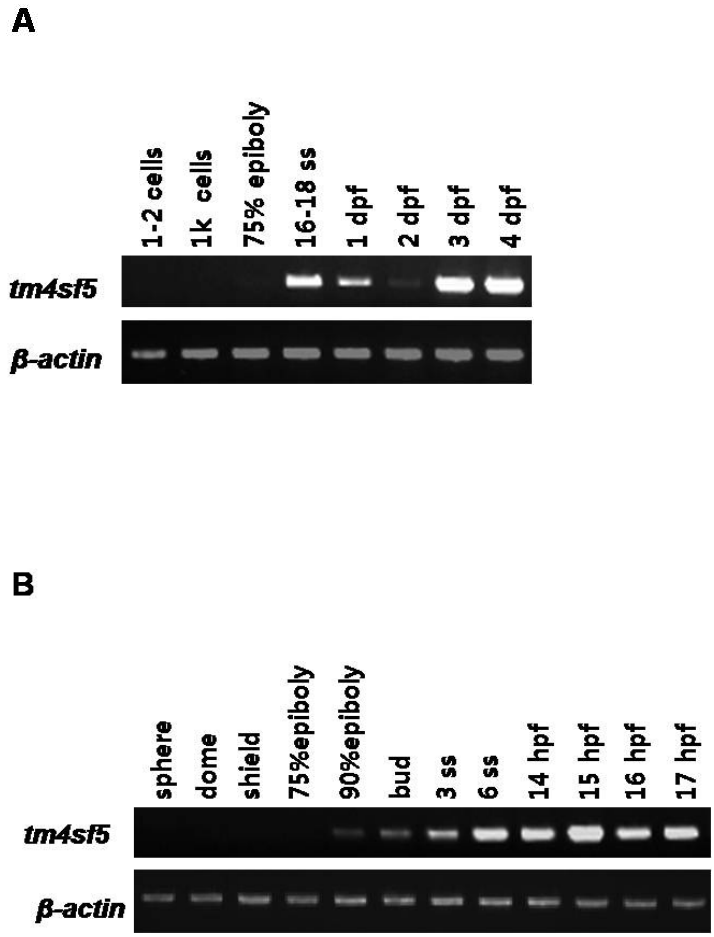

Figure 2. *tm4sf5* mRNA expression level showed several peaks.

(A) RT-PCR analysis of *tm4sf5* mRNA during overall embryogenesis (B) RT-PCR analysis of *tm4sf5* mRNA for detailed time-wise analysis, in the period between sphere stage and 17 hpf. Abbreviation: ss, somites stage; hpf, hours post fertilization.

2.2 Spatio-temporal expression pattern of *tm4sf5* during embryogenesis

Next we investigated the spatio-temporal expression pattern of *tm4sf5* using whole mount *in situ* hybridization. At the early time of somitogenesis, *tm4sf5* was expressed throughout the whole embryo (Fig. 3A). In the middle of somitogenesis stage, however, *tm4sf5* expression became more distinct in the posterior somites of trunk region (Fig 3B,C,D). It was also found in head. After 1 dpf, *tm4sf5* was expressed in the entire myotome, notochord, neural tubes, and head. (Figs. 3E, F, G, and H). The entire expression level of *tm4sf5* was decreased at 2 dpf in accordance with RT-PCR observation but maintained slightly in notochord (Fig 3I). After 3 and 4 dpf, the expression of *tm4sf5* was found in notochord and head (Figs. 4A, B, D, and E) and especially highly expressed in gut tube (Fig 4C,D). Because the most of developmental changes in embryonic morphology occur until 2 dpf (15), the elevated expression of tm4sf5 until 1 dpf suggested that tm4sf5 might have a role in zebrafish morphogenesis. Based on the observations that tm4sf5 transcripts were detected in somites and the entire myotome, we speculated that tm4sf5 functions in period throughout somitogenesis and myogenesis.

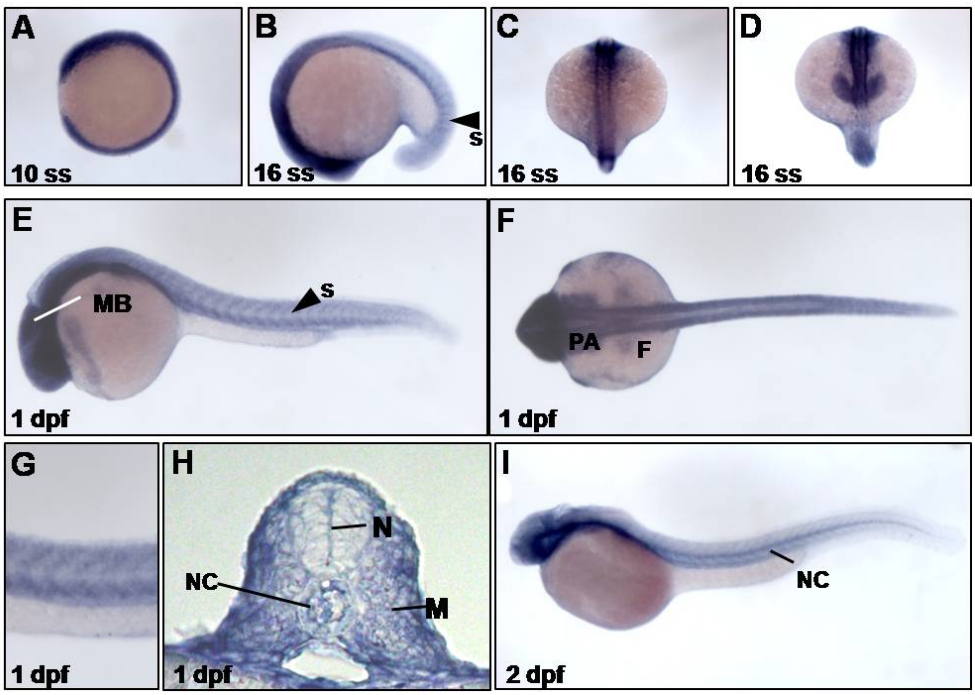

Figure 3. Expression pattern of *tm4sf5* during early embryogenesis.

Whole mount *in situ* hybridization analysis using a full-length *tm4sf5* probe of zebrafish embryos. Stained embryos were viewed from left lateral (A, B, E, G, and I) dorsal (C, F), and ventral (D). (H) is a transverse section of stained embryos. Expression of *tm4sf5* was detected thoughout the whole embryos until 10-somite stage (A). During somitogenesis stage, expression of *tm4sf5* was detected at head and somites (B,C,D ; Arrowhead Indicated). After 1 dpf, *tm4sf5* was expressed in the whole myotome, head , pharyngeal arches, neural tube and notochord (H). Abbreviation: ss, somites stage; s, somites; mb, midbrain; pa, pharyngeal arches; f, fin bud; n, neural tube; nc, notochord; m, myotome.

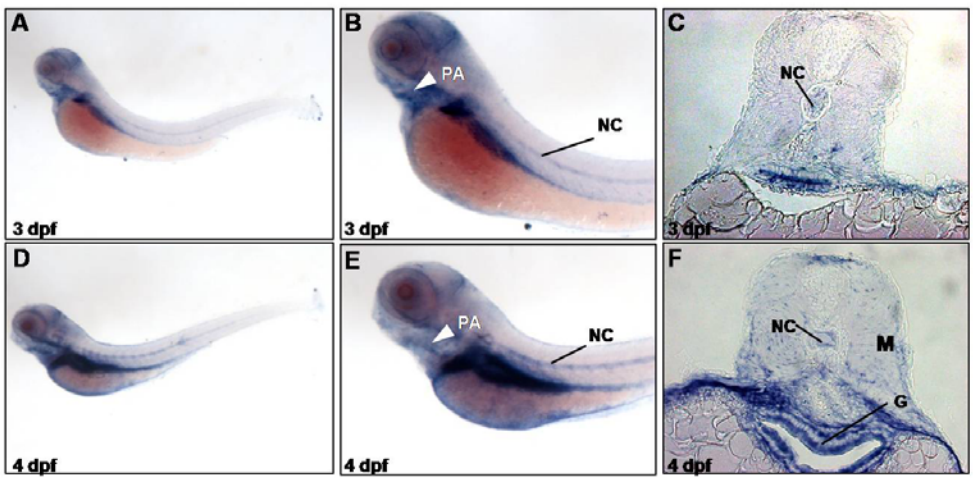

Figure 4. Expression pattern of *tm4sf5* during late embryogenesis.

Stained embryos were viewed from lateral (A, B, D, and E). *tm4sf5* mRNA was expressed in head, notochord and gut tube at 3 dpf and 4 dpf (A, B, C, D, E, and F). Transverse section of stained embryos showed *tm4sf5* transcripts at notochord and gut tube (C, F). Abbreviation: g-gut tube.

3. Knock-down of *tm4sf5* by antisense morpholino oligonucleotides

3.1 The validation of antisense morpholino oligonucleotides

To study the function of *tm4sf5*, we interfered with its expression using two different mopholino oligonucleotides, which were targeted to the translation-initiation site (trs MO, data not shown) or the splice donor site (spl MO). The spl MO was designed to target the exon 1-intron 1 boundary (Fig 5A). After microinjection of the MOs into the embryos at 1-4 cell stage, we selected embryos after 4 dpf and performed RT-PCR analysis to assess the efficiency of *tm4sf5* knockdown. Using primers to detect the full-length *tm4sf5* (F1 and R3; a product of 629 bp), exon1 to exon2 of *tm4sf5* (F1 and R2; a product of 398 bp), we confirmed that the expression of *tm4sf5* was suppressed efficiently (Fig 5B). Aberrantly spliced product was also detected using intron-specific primers (F1 and R1; a product of 363 bp) (Fig 5B). Next we performed *in situ* hybridization using 1 dpf control and morphants microinjected with spl MO to reconfirm the suppression of *tm4sf5*. The expression of *tm4sf5* in morphants was decreased in head and trunk region, compared with control embryos (Fig 5C). Based on these observations, we successfully confirmed that the knock-down of *tm4sf5* using anti-sense morpholino oligonucleotides was functional.

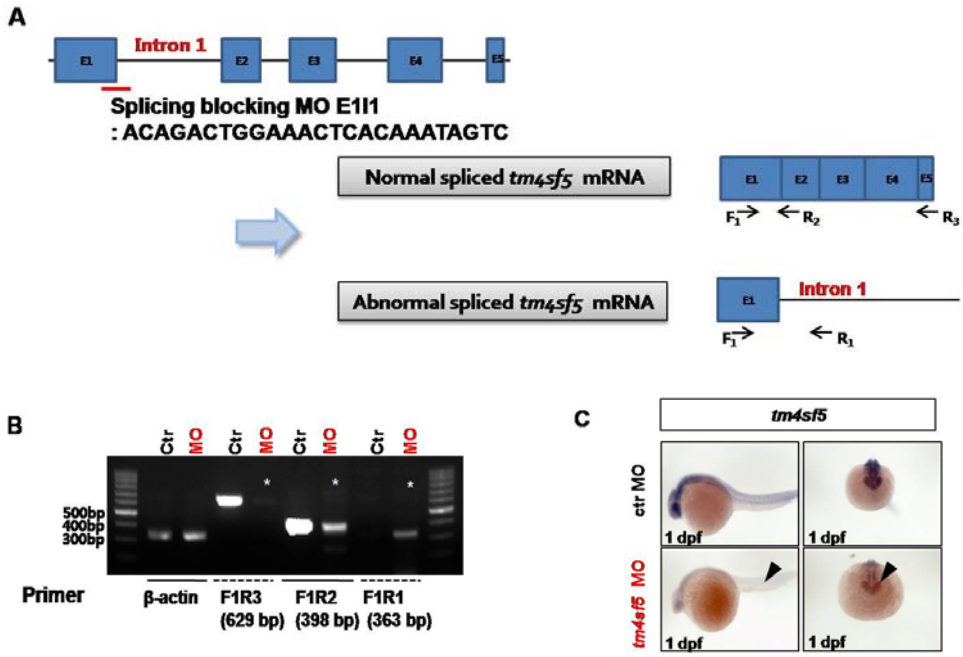

Figure 5. Knock-down of *tm4sf5* by antisense morpholino oligonucleotides

(A) The scheme of splice-blocking MO. The MO was designed to target the boundary between *tm4sf5* exon 1 and intron 1. (B) RT-PCR analysis to determine the effect of *tm4sf5* MO. Total mRNA was isolated from control and *tm4sf5* morphant embryos at 4 dpf. Morphants showed abnormally spliced *tm4sf5* mRNA that had intron sequences inserted. (F1 and R1; a product of 363 bp). (C) Expression of *tm4sf5* was decreased in *tm4sf5* morphant embryos compared with control embryos**.**

3.2 Knock-down of *tm4sf5* induced defect in head, trunk, and cardiac development

We then investigated the phenotypes of morphants induced by loss of *tm4sf5* function. Similar phenotypes including small head, embryonic heart failure, and curved trunk were induced by injection of trs MO or spl MO. Because small head, pericardial edema were appeared in the majority of morphants regardless of the dose injected, the phenotypes of *tm4sf5* morphants were classified by the degree of defect provoked in trunk after 4 dpf (Fig 6A). The severity of defect in trunk was proportionally increased as the concentration of trs MO or spl MO was increased (Fig 6B,C). From these data we could conclude that knock-down of *tm4sf5* inhibited overall development of head, trunk, and heart in zebrafish embryos. But because only the tail morphology was induced dose-dependently among these phenotypes, we could infer that *tm4sf5* might functionally affect the formation of trunk and tail. And the optimal dose of MO used in this study was fixed as 2ng/embryo at which the defect of embryonic morphology was not too much severe.

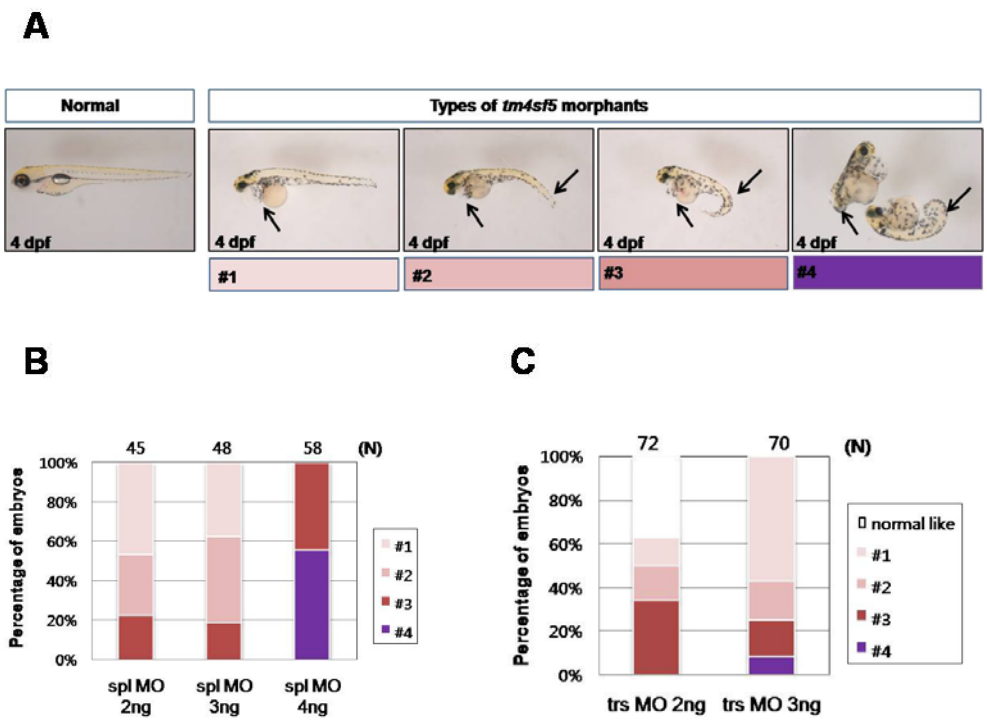

Figure 6. Knock-down of *tm4sf5* induced defect in head, trunk, and cardiac development.

(A) Several types of defects were induced in tm4sf5 morphant embryos by microinjection of *tm4sf5* MO in lateral views. All types of morphants showed small head and pericardial edema. Type 1 (#1) embryos showed pericardial edema and reduced head size. Type 2 (#2) embryos showed pericardial edema, small head, and slightly curved trunk. Type 3 (#3) and Type 4 (#3) showed the most defects in trunk and short body length. Arrows indicated defects in trunk and heart morphology. As the number for the type increase, the defects become more severe. (B) and (C) showed graphic depiction of percentage of embryos with 4 types of phenotypes. The severity of defect in trunk morphology was proportional to the amount of *tm4sf5* spl MO (B), and *tm4sf5* trs MO (C).

4. Expression pattern of myogenic progenitor cell marker in control and *tm4sf5* morphant embryos

In adult zebrafish, the trunk structure is composed of muscle, cartilage and bone derived from somites (13). The somites give rise to the myotome mainly during somitogenesis at the first day of development (13). Several data above revealed that *tm4sf5* was expressed in the somites during somitogenesis and in the entire myotome at the end of somitogenesis. Further, loss of *tm4sf5* function affected trunk morphology of the morphants. In addition, the morphants were not able to swim straight forward, swirling in response to a touch (data not shown). Therefore, we hypothesized that *tm4sf5* might function in the formation of the somites and myotome, including development of muscle fibers.

We thus tested whether the differentiation of myogenic progenitor cells was normal. *Myogenic differentiation* (*myoD*) is known to be expressed in muscle progenitor cell from the onset of the somitogenesis (16). Using *in situ* hybridization analysis, we found that expression of *myoD* in *tm4sf5* morphants was not affected in the several stages of somitogenesis, compared with control MO-injected embryos (Fig 7 A-F). Based on these observations, it is likely that *tm4sf5* may not affect the formation and patterning of somites. After 1 dpf at which somite formation was nearly over, however, expression of *myoD* was altered in morphants (Fig 7G-L). The area of cells expressing *myoD* was reduced in morphants, compared with control MO-injected embryos, and segments of formed somite were not clearly separated, compared with control embryos. Therefore aberrant trunk and tail morphology in morphants was not correlated with the formation of somites,

but more correlated with the processes in which already-formed somites differentiated into muscle fiber types.

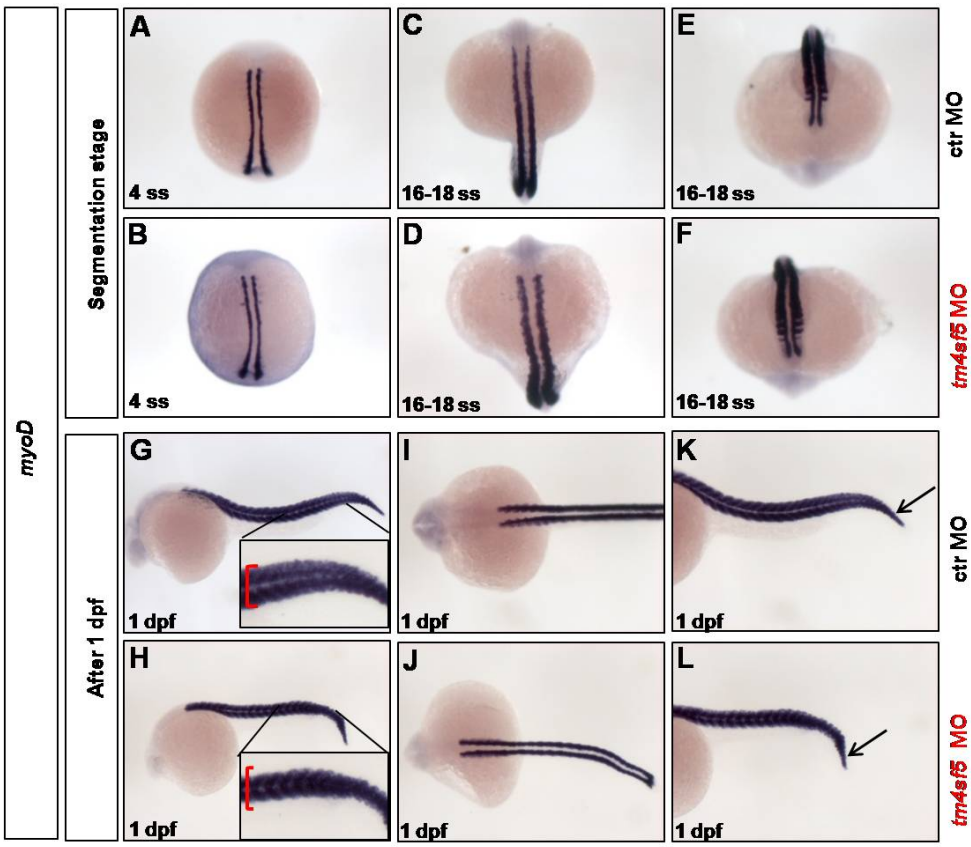

Figure 7. Expression pattern of myogenic progenitor cell marker in control and *tm4sf5* morphant embryos.

Expression of *myoD* was not changed during sementation stages in *tm4sf5* morphant embryos (A-F). After 1 dpf, however, *myoD*-expressing areas were severely reduced and expression pattern in trunk was altered in morphant embryos (G-L). Dorsal views; (A-D), Dorso-posterior views; (E-F), Lateral views; (G-H), Dorso-anterior views; (I-J), Lateral-posterior views; (K-L) Arrows indicated abnormal trunk and tail morphology in morphants compared with control embryos.

5. Slow muscle and fast muscle development in control and *tm4sf5* morphant embryos

During somitogenesis, *myoD*-expressing muscle progenitor cells begin to differentiate into two different types of muscle fibers (17). The more medially positioned adaxial cells migrate away from the notochord to become superficial slow muscle fiber, as other cells differentiate into fast muscle fiber in the deep portion of myotome (13). We thus tested whether loss of *tm4sf5* function affected formation of muscle fibers. Using antibodies that recognize myosin heavy chain in slow and fast muscle fiber, we found that both muscle types were morphologically abnormal in morphants (Fig. 8). The overall muscle mass was reduced in morphants, compared with control embryos (Fig. 8A). While the slow muscle cells migrated properly to the superficial region of myotome and formed parallel stacks of fibers, there were spaces where the fibers were missing in dorsal and ventral regions of morphant embryos and muscle pioneer cells in the midline of the embryos were abnormally distributed (Figs. 8B, C, and D). In case of fast muscle, fibers were missing in dorsal and ventral regions of morphants, compared with control embryos (Figs. 8E, G, F, and H). We can thus conclude that knock-down of *tm4sf5* induced morphogenetic defects in the both muscle fiber types, including reduced muscle masses. These data suggest that *tm4sf5* may be involved in the morphogenesis of muscle fibers.

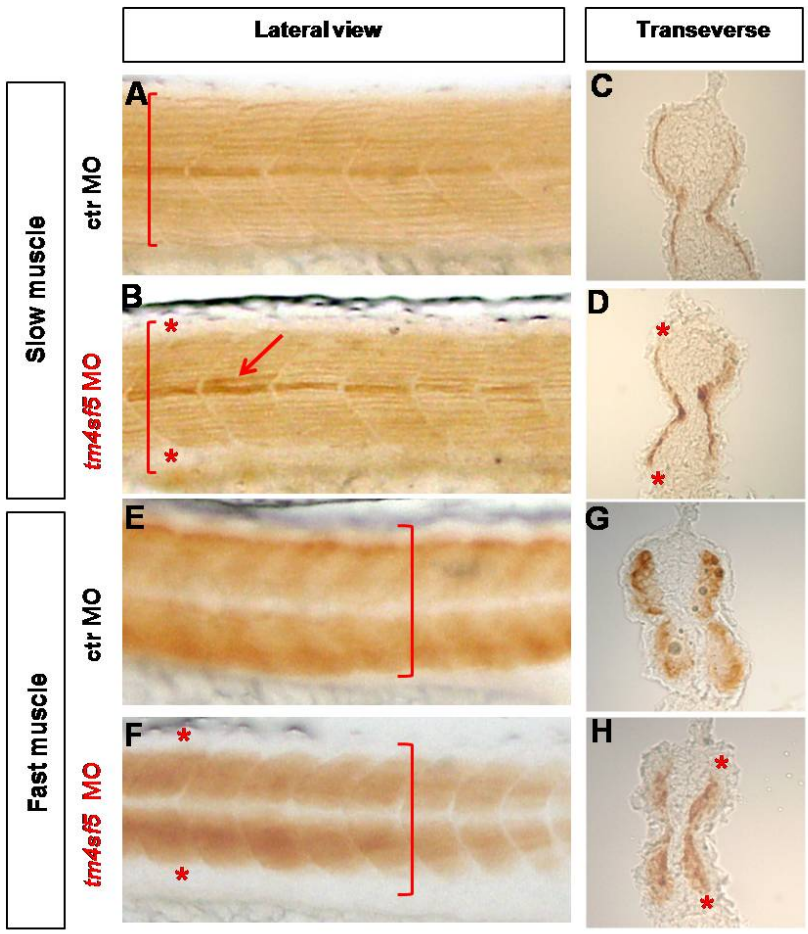

Figure 8. Slow muscle and fast muscle fiber development in *tm4sf5* morphant embryos.

Images of control (A,C,E,G) and morphant embryos (B, D, F, and H) after 1 dpf in lateral views (A, B, E, and F), and in transverse section (C, D, G, and H). Embryos were immunostained with F59 antibody to detect slow muscle fibers (A-D), and with F310 antibody to detect fast muscle fibers (E-H). Asterisks indicated where slow muscle and fast muscle fibers were missing. Arrow indicated abnormal distribution of muscle pioneer cells in *tm4sf5* morphants.

6. Altered expression pattern of *integrin* α5 in *tm4sf5* morphant embryo

Next we investigated the factors that affect the morphogenesis of muscle fibers. It has been proposed that muscle fibers are formed as somitic cells elongate into long fiber type cells, anchoring to intersegmental boundaries (19). Therefore, the proper formation of the boundaries is important for morphogenesis of muscle fibers. Importantly, the focal adhesion components, such as FAK and paxillin, have been shown to be accumulated at the intersomitic borders and act as adaptor proteins during cell engagement via an interaction between integrins and extracellular matrix (21). Especially *integrin α5*-dependent fibronectin accumulation at the boundaries has been shown to be required for maintenance of intersomitic boundaries of posterior somites (22). Because previous studies demonstrate that TM4SF5 cooperates with integrin α5 to regulate cell adhesion and migration in human cells (2), we hypothesized that *tm4sf5* might affect the zebrafish myogenesis through interaction with *integrin α5*. Using *in situ* hybridization analysis, we determined that expression of *integrin α5* was altered in *tm4sf5* morphant embryos, compared with control embryos. *Integrin α5* was expressed in many parts of wild type embryos including muscle pioneers and branchial arches after 1 dpf (Figs. 9A, C, and E). However in *tm4sf5* morphant embryos, the overall expression of *integrin α5* was disrupted and spread out in the whole embryo including yolk syncytial layers (Figs. 9B, D, and F). The expression in the pharyngeal arches was reduced in morphants (Fig. 9D). Further importantly, the expression of *integrin α5* in the muscle pioneer cells was spread out dorsally and

ventrally in the morphant embryos, not in the exact position (Figs. 9B, and F). Muscle pioneer cell is a kind of slow muscle cell type, and the alteration of the expression of *integrin α5* in these cells coincided with disruption of slow muscle fiber, as shown in figure 8B. These results support our hypothesis that *tm4sf5* cooperate with *integrin α5* during zebrafish myogenesis.

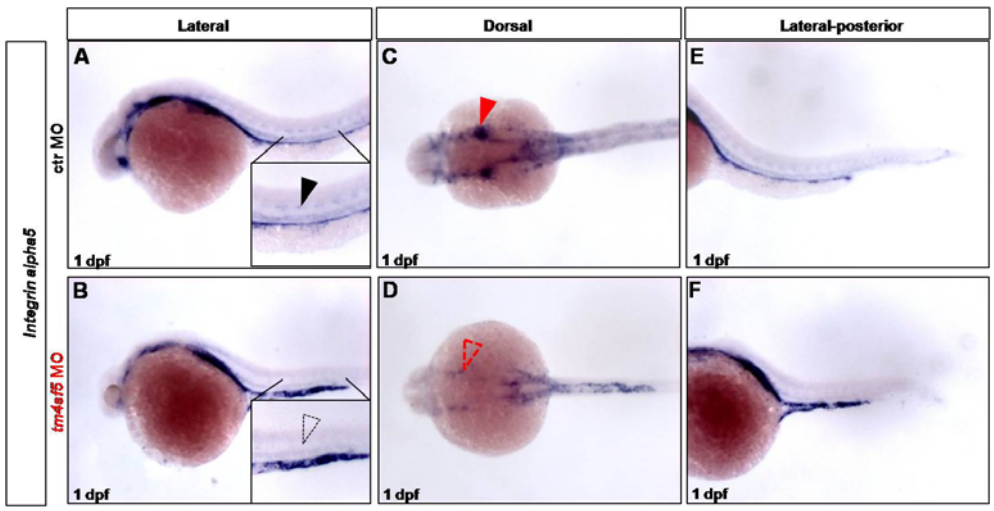

Figure 9. Altered expression pattern of *integrin α5* in *tm4sf5* morphant embryos.

Expression patterns of integrin α5 in muscle pioneer cells were altered in morphant embryos, spreading out in the dorsal and ventral region of the embryos (A-B ; black arrowhead indicated in the boxes). In pharyngeal arches, the expression pattern was reduced in *tm4sf5* morphants compared with control embryos (C-D; red arrowhead indicated) and appeared more in yolk syncytial layers, not in exact position (E-F; black arrow indicated). Lateral views; (A, B), Dorso-anterior views; (C, D), Lateral-posterior views; (E, F)

Discussion

This study presents the first functional analysis of *tm4sf5* in zebrafish development. We observed that *tm4sf5* was highly expressed in somites and myotome during somitogenesis. The knock-down of *tm4sf5* impaired development of trunk and tail and showed abnormal morphology of muscle fibers, suggesting the regulatory role of tm4sf5 in myogenesis. The expression of *integrin α5* was further altered by the knock-down of tm4sf5. Thus we speculate that *tm4sf5* functions as a regulator of myogenesis via cooperation with *integrin α5*. Previous studies revealed that TM4SF5 functions as a key modulator in communication between tumor cells and tumor microenvironment, regulating cell migration and EMT via interaction with signaling molecules as FAK, integrin receptors, and growth factor receptors (1, 4-7). Because the proper regulation of cell migration and EMT process is crucial for normal development during embryonic morphogenesis (9), it was inferred possible that zebrafish *tm4sf5* also play important roles as a regulator in developmental processes.

We identified that TM4SF5 is conserved in zebrafish as well as other vertebrates and the intracellular loop domain of TM4SF5 which binds FAK is highly conserved in zebrafish. TM4SF5 directly binds FAK leading to FAK activation and enhanced cell migration in hepatocytes (5). This suggested that zebrafish TM4SF5 might also play similar roles via interaction with FAK. *fak* mRNA is expressed in developing somites and Fak protein localizes at intersegmental boundaries in zebrafish as myotome matures (20). We found that *tm4sf5* mRNA expression was

elevated during somitogenesis, and was also detected in developing somites, like *fak* mRNA. This coincidence supports our hypothesis that *tm4sf5* may have potential role in cell behaviors correlated with *fak*. Our observation that *tm4sf5* mRNA expression was increased until 1 dpf and dramatically decreased after 2 dpf also suggests the possibility that t*m4sf5* is likely to act in the period important for somitogenesis and myogenesis, which occur usually within 1 dpf.

A role of *tm4sf5* in the developmental regulation during somite and myotome formation could be reinforced by knock-down study using antisense morpholino oligonucleotides. We observed that the knock-down of *tm4sf5* impaired normal development of head, heart, and trunk in zebrafish. *tm4sf5* morphants displayed small head, pericardial edema, and curved trunk. Especially only in trunk, the impaired phenotype got worse dose-dependently. The morphants displayed signs of myopathy, such as overall reduction of muscle mass and disarray of muscle fibers. Similar phenotypes have previously been observed in many other genes acting in different cellular pathways (29-33). These defects were not caused by the early differentiation of myogenic progenitor cells but by malformation of the myofibers because the expression of myogenic transcription factor *myoD* was not altered in morphants.

During somitogenesis, specification of the slow muscle precursor begins with the onset of myogenesis (13). Muscle progenitors expressing myogenic transcription factors begin to differentiate into muscle fibers (16). In this process, a wide range of cell migration occurs. Adaxial cell populations which are adjacent to notochord move toward the lateral surface of the myotome, simultaneously changing cell shape into long and skinny rod shape (13). A few of adaxial cells remain adjacent

to notochord, composing of muscle pioneers (17). The more lateral paraxial cell populations differentiate into fast muscle fibers (13). The signaling molecules involved in specifying slow and fast muscle cell fate are proteins like Sonic Hedgehog and BMPs (34). Our observation showed that the specification of slow and fast muscle was not affected as shown by the normally positioned muscle fibers in transverse sections. However, the morphology of muscle fibers was abnormal in *tm4sf5* morphants, indicated by disarray of muscle fibers and reduced overall mass. Therefore, these observations suggest *tm4sf5* function(s) in the other underlying mechanism in myotome formation, which may appear to involve migration capacity of muscle progenitor cells for differentiation into slow and fast muscle cells, as shown in the hepatocyte leading to enhanced migration (5). It will be important to study migration and fusion of muscle precursor cells by time-lapse imaging analysis.

Once the muscle fibers elongate, they attach strongly to the myotome boundary (35). The myotome boundary is more mature structure derived from initial somite boundary (36). The improper boundary formation induces abnormal morphology of muscle fibers (19). There are dystrophin-associated glycoprotein complex, integrin receptors, and focal adhesion molecules as linkage systems between the muscle cytoskeleton and extracellular matrix (ECM) in myotome boundary (36). When the strong adhesion between muscle cells and ECM is formed at boundary sites, the activated Fak indicated by phorphorylation of Tyr^{397} is accumulated (21). This indicates that the integrin signaling is activated at these sites. In previous studies, TM4SF5 is also known to interact with integrins and act as a modulator of downstream signaling molecules like FAK and Src (1, 3-6) (and Choi et al, in

revision). As mentioned above, TM4SF5 binds FAK and regulates the activity (5). Thus, it could be likely that the function of *tm4sf5* in zebrafish might be a modulator of these molecules in myotome formation, presumably also via collaborations with integrins.

Integrin α5, a subunit of fibronectin receptor, has been shown to regulate cell migration and adhesion in human cells, retained at cell surfaces by TM4SF5 being complexed (2). It is proposed that integrin α5-directed assembly of fibronectin matix is necessary for epithelialization of somitic border cells and somite boundary maintenance in zebrafish (22). In this study, we observed that when *tm4sf5* was functionally impaired in *tm4sf5* morphants, the expression of *integrin α5* was altered. The expression pattern of *integrin α5* in muscle pioneers was disrupted and spread out dorsally and ventrally in morphants, suggesting that the disarray of muscle pioneers in slow muscle fibers resulted from this disruption of *integrin α5*. These observations support our hypothesis that *tm4sf5* function as a signaling modulator during myotome formation, regulating the function and/or expression of *integrin α5*. Because the focal adhesion proteins, integrin receptors and ECM molecules form the myotome boundary in coordination with each other, the alteration of *integrin α5* expression or function by *tm4sf5* may affect other components in focal adhesions and/or integrin-downstream molecules (36). To see whether it is the case, the molecules should be studied further.

In summary, we found that when *tm4sf5* was downregulated in zebrafish, normal trunk development was impaired dramatically and the morphology of muscle fibers was abnormal, indicating malformation of myotome, with altered expression of *integrin α5* in muscle pioneers by knock-down of *tm4sf5*. From all observations in

this study, we can speculate that *tm4sf5* performs a regulatory role via cooperation with integrin α5 in developmental process especially during myotome formation.

References

1. Lee SY, Kim YT, Lee MS, Kim YB, Chung E, Kim S, et al. Focal adhesion and actin organization by a cross-talk of TM4SF5 with integrin α2 are regulated by serum treatment. Experimental cell research. 2006 Oct 1;312(16):2983-99.
2. Choi S, Lee SA, Kwak TK, Kim HJ, Lee MJ, Ye SK, et al. Cooperation between integrin α5 and tetraspan TM4SF5 regulates VEGF-mediated angiogenic activity. Blood. 2009 Feb 19;113(8):1845-55.
3. Lee SA, Kim YM, Kwak TK, Kim HJ, Kim S, Ko W, et al. The extracellular loop 2 of TM4SF5 inhibits integrin α2 on hepatocytes under collagen type I environment. Carcinogenesis. 2009 Nov;30(11):1872-9.
4. Lee SA, Kim TY, Kwak TK, Kim H, Kim S, Lee HJ, et al. Transmembrane 4 L six family member 5 (TM4SF5) enhances migration and invasion of hepatocytes for effective metastasis. Journal of cellular biochemistry. 2010 Sep 1;111(1):59-66..
5. Jung O, Choi S, Jang SB, Lee SA, Lim ST, Choi YJ, et al. Tetraspan TM4SF5-dependent direct activation of FAK and metastatic potential of hepatocarcinoma cells. Journal of cell science. 2012 Oct 17.
6. Lee SA, Lee SY, Cho IH, Oh MA, Kang ES, Kim YB, et al. Tetraspanin TM4SF5 mediates loss of contact inhibition through epithelial-mesenchymal transition in human hepatocarcinoma. The Journal of clinical investigation. 2008 Apr;118(4):1354-66.
7. Kang M, Choi S, Jeong SJ, Lee SA, Kwak TK, Kim H, et al. Cross-talk between TGFβ1 and EGFR signalling pathways induces TM4SF5 expression and epithelial-mesenchymal transition. The Biochemical journal. 2012 May 1;443(3):691-700.
8. Lee JM, Dedhar S, Kalluri R, Thompson EW. The epithelial-mesenchymal transition: new insights in signaling, development, and disease. The Journal of cell biology. 2006 Mar 27;172(7):973-81.
9. Moustakas A, Heldin CH. Signaling networks guiding epithelial-mesenchymal transitions during embryogenesis and cancer progression. Cancer science. 2007 Oct;98(10):1512-20.
10. Kang M, Jeong SJ, Park SY, Lee HJ, Kim HJ, Park KH, et al. Antagonistic regulation of transmembrane 4 L6 family member 5 attenuates fibrotic phenotypes in CCl_4 -treated mice. The FEBS journal. 2012 Feb;279(4):625-35.
11. Schmidt JW, Piepenhagen PA, Nelson WJ. Modulation of epithelial morphogenesis and cell fate by cell-to-cell signals and regulated cell adhesion. Seminars in cell biology. 1993 Jun;4(3):161-73.
12. Hollway G, Currie P. Vertebrate myotome development. Birth defects research Part C, Embryo today : reviews. 2005 Sep;75(3):172-9.

13. Stickney HL, Barresi MJ, Devoto SH. Somite development in zebrafish. Developmental dynamics : an official publication of the American Association of Anatomists. 2000 Nov;219(3):287-303.
14. Fishman MC, Stainier DY, Breitbart RE, Westerfield M. Zebrafish: genetic and embryological methods in a transparent vertebrate embryo. Methods in cell biology. 1997;52:67-82.
15. Kimmel CB, Ballard WW, Kimmel SR, Ullmann B, Schilling TF. Stages of embryonic development of the zebrafish. Developmental dynamics : an official publication of the American Association of Anatomists. 1995 Jul;203(3):253-310.
16. Buckingham M, Vincent SD. Distinct and dynamic myogenic populations in the vertebrate embryo. Current opinion in genetics & development. 2009 Oct;19(5):444-53.
17. Devoto SH, Melançon E, Eisen JS, Westerfield M. Identification of separate slow and fast muscle precursor cells in vivo, prior to somite formation. Development. 1996;122.
18. Henry CA, Amacher SL. Zebrafish slow muscle cell migration induces a wave of fast muscle morphogenesis. Developmental cell. 2004 Dec;7(6):917-23.
19. Henry CA, McNulty IM, Durst WA, Munchel SE, Amacher SL. Interactions between muscle fibers and segment boundaries in zebrafish. Developmental biology. 2005 Nov 15;287(2):346-60.
20. Henry CA, Crawford BD, Yan YL, Postlethwait J, Cooper MS, Hille MB. Roles for zebrafish focal adhesion kinase in notochord and somite morphogenesis. Developmental biology. 2001 Dec 15;240(2):474-87.
21. Crawford BD, Henry CA, Clason TA, Becker AL, Hille MB. Activity and distribution of paxillin, focal adhesion kinase, and cadherin indicate cooperative roles during zebrafish morphogenesis. Molecular biology of the cell. 2003 Aug;14(8):3065-81.
22. Koshida S, Kishimoto Y, Ustumi H, Shimizu T, Furutani-Seiki M, Kondoh H, et al. Integrin α5-dependent fibronectin accumulation for maintenance of somite boundaries in zebrafish embryos. Developmental cell. 2005 Apr;8(4):587-98.
23. Hemler ME. Tetraspanin functions and associated microdomains. Nature reviews Molecular cell biology. 2005 Oct;6(10):801-11.
24. Hemler ME. Targeting of tetraspanin proteins--potential benefits and strategies. Nature reviews Drug discovery. 2008 Sep;7(9):747-58.
25. Anderson KR, Singer RA, Balderes DA, Hernandez-Lagunas L, Johnson CW, Artinger KB, et al. The L6 domain tetraspanin Tm4sf4 regulates endocrine pancreas differentiation and directed cell migration. Development. 2011 Aug;138(15):3213-24.
26. Weinberg ES, Allende ML, Kelly CS, Abdelhamid A, Murakami T,

Andermann P, et al. Developmental regulation of zebrafish MyoD in wild-type, no tail and spadetail embryos. Development. 1996 Jan;122(1):271-80.
27. Thisse C, Thisse B. High-resolution in situ hybridization to whole-mount zebrafish embryos. Nature protocols. 2008;3(1):59-69.
28. Moulton JD, Yan YL. Using Morpholinos to control gene expression. Current protocols in molecular biology / edited by Frederick M Ausubel [et al]. 2008 Jul;Chapter 26:Unit 26 8
29. Raeker MO, Russell MW. Obscurin depletion impairs organization of skeletal muscle in developing zebrafish embryos. Journal of biomedicine & biotechnology. 2011;2011:479135.
30. Snow CJ, Peterson MT, Khalil A, Henry CA. Muscle development is disrupted in zebrafish embryos deficient for fibronectin. Developmental dynamics : an official publication of the American Association of Anatomists. 2008 Sep;237(9):2542-53.
31. Lobbardi R, Lambert G, Zhao J, Geisler R, Kim HR, Rosa FM. Fine-tuning of Hh signaling by the RNA-binding protein Quaking to control muscle development. Development. 2011 May;138(9):1783-94.
32. Ahmed H, Du SJ, Vasta GR. Knockdown of a galectin-1-like protein in zebrafish (Danio rerio) causes defects in skeletal muscle development. Glycoconjugate journal. 2009 Apr;26(3):277-83.
33. Nixon SJ, Wegner J, Ferguson C, Mery PF, Hancock JF, Currie PD, et al. Zebrafish as a model for caveolin-associated muscle disease; caveolin-3 is required for myofibril organization and muscle cell patterning. Human molecular genetics. 2005 Jul 1;14(13):1727-43.
34. Maurya AK, Tan H, Souren M, Wang X, Wittbrodt J, Ingham PW. Integration of Hedgehog and BMP signalling by the engrailed2α gene in the zebrafish myotome. Development. 2011 Feb;138(4):755-65.
35. Snow CJ, Henry CA. Dynamic formation of microenvironments at the myotendinous junction correlates with muscle fiber morphogenesis in zebrafish. Gene expression patterns : GEP. 2009 Jan;9(1):37-42.
36. Charvet B, Malbouyres M, Pagnon-Minot A, Ruggiero F, Le Guellec D. Development of the zebrafish myoseptum with emphasis on the myotendinous junction. Cell and tissue research. 2011 Dec;346(3):439-49.

요 약

Transmembrane 4 L6 family member 5 (TM4SF5) 는 tetraspanin superfamily 에 속하는 막단백질로서, 세포막을 네 번 통과하는 구조를 갖고 있는 당단백질이다. TM4SF 는 다른 tetraspanin, 성장인자 수용체, integrin 등과 함께 tetraspanin-enriched microdomains (TEM) 을 형성하여 그 기능을 수행할 것이라고 추정되고 있다. 선행 연구들에서, TM4SF5 는 세포 수준에서 EMT (epithelial-mesenchymal transition, 상피-중배엽세포 전이)을 유발함으로써 세포의 형태 변화뿐 아니라 이동과 침윤, 증식을 촉진하는 역할을 하고 있음이 밝혀졌다.

한편, 척추동물의 배아 발달과정은 세포의 형태 변화, 이동 등이 동시다발적으로 일어나는 복잡한 과정이다. 선행 연구들에서 밝혀진 TM4SF5 의 생물학적 기능에 바탕하여 TM4SF5 가 EMT 나 세포 이동에 관여함으로써 배아 발달과정에 일정 역할을 수행할 것이라는 가설이 가능하였기에, 본 논문은 TM4SF5 의 발달과정 상에서의 기능을 제브라피쉬 실험모델동물을 통하여 알아보고자 하였다.

제브라피쉬에서 수정 후 1 일 이내에 중배엽 세포는 체절로 분화되며, 체절을 이루는 세포의 대부분은 근절을 형성하게 된다. *tm4sf5* mRNA 의 발현을 확인해본 결과, 수정 후 10 시간에서 24 시간 사이의 시기에 배아 후방부위의 체절에서 발현하였고, 24 시간 이후 근절 전체부위에 나타나는 양상을 보였다. Antisense morpholino oligonucleotide 를 이용하여 *tm4sf5* 를 knockdown 한 결과 제브라피쉬 배아에서 꼬리 부위의 비정상적인 발달과 움직임의 저해가 나타났다. 이러한 결과는 *tm4sf5* 가 제브라피쉬 근육 발달에 중요한 역할을 할 것이라고 추정되었다. 또한 *tm4sf5*-knockdown 배아에서 제브라피쉬의 근육 전구체에서 발현하는 유전자인 *myogenic differentiation* (*myoD)*

가 수정 후 24 시간이 지난 시점에 비정상적으로 발현하는 것을 확인하였고, 지근섬유와 속근섬유가 비정상적으로 형성되는 것을 확인하였다. 즉, 대조군 배아에 대비하여 *tm4sf5*-knockdown 배아에서, 전체적인 근육의 부피가 줄어들었고 지근섬유와 속근섬유의 분포가 불규칙적으로 나타났다. 그리고 이 *tm4sf5*-knockdown 배아들에서 근절 경계의 형성에 관여하며 지근섬유 전구체 세포에서 나타나는 *integrin a5* 의 발현양상이 변화된다는 것을 확인하였다. 이를 통해 *tm4sf5* 가 제브라피쉬의 발달 과정에 관여하고 있으며, *integrin a5* 를 조절함으로써 근육 세포의 정상적인 분화에 기여하고 있다는 가능성을 제시하였다.

주요어 : 발달과정, TM4SF5, 제브라피쉬, 체절, 근육, integrin α5
학번 : 2011-21775